



Low Loss Regrowth-Free Long Wavelength Quantum Cascade Lasers

Journal:	<i>Photonics Technology Letters</i>
Manuscript ID	PTL-34734-2018
Manuscript Type:	Original Paper
Date Submitted by the Author:	28-May-2018
Complete List of Authors:	Gundogdu, Sinan; Bilkent Universitesi Fen Fakultesi, Physics Department Demir, Abdullah; Bilkent Universitesi, Physics Sedaghat Pisheh, Hadi; Bilkent Universitesi Makine Muhendisligi Bolumu, mechanical engineering Aydinli, Atilla ; Uludağ University, Electrical and Electronics Engineering
Key Words:	quantum cascade lasers, quantum efficiency, Optical losses, Hafnium, Passivation, Quantum well lasers, Semiconductor device fabrication, Laser modes, Semiconductor lasers

SCHOLARONE™
Manuscripts

Low Loss Regrowth-Free Long Wavelength Quantum Cascade Lasers

Sinan Gündoğdu, Abdullah Demir, Hadi Sedaghat Pisheh, Atilla Aydınli

Abstract—Optical power output is the most sought-after quantity in laser engineering. This is also true of quantum cascade lasers operating especially at long wavelengths. Buried heterostructure cascade lasers with epitaxial regrowth have typically shown the lowest loss due to high current confinement as well as superior lateral thermal conductivity at the expense of complexity and cost. Among the many factors affecting optical output are the widely used passivating materials such as Si_3N_4 and SiO_2 . These materials have substantial optical absorption in the long wave infrared, which result in optical loss reducing the output of the laser. In this study, we report on quantum cascade lasers with various waveguide widths and cavity lengths using both PECVD grown Si_3N_4 and e-beam evaporated HfO_2 as passivating material on the same structure. Their slope efficiency was measured and the cavity loss for the two lasers were calculated. We show that HfO_2 passivated lasers have approximately 5.5 cm^{-1} lower cavity loss compared to Si_3N_4 passivated lasers. We observe up to 38% reduction in lasing threshold current, for lasers with HfO_2 passivation. We model the losses of the cavity due to both insulator and metal contacts of the lasers using Comsol Multiphysics for various widths. We find that the loss due to absorption of dielectric is a significant effect for Si_3N_4 passivated lasers and lasers at 8-12 μm range may benefit from low loss passivation materials such as HfO_2 . Our results suggest that low loss long wavelength quantum cascade lasers can be realized without epitaxial overgrowth.

Index Terms—Quantum cascade lasers, quantum efficiency, loss, hafnium dioxide, passivation.

I. INTRODUCTION

Quantum cascade lasers (QCLs) are unique devices that emit coherent light in a wide spectrum from near-infrared to terahertz frequencies. Their optical output has increased dramatically in the past 20 years from a few mW to several Watts for some wavelength ranges. The requirements of high optical power is ever more present, especially as the lasing wavelength gets longer. In addition to optimization of design and epitaxial growth parameters, the technologies used to fabricate lasers need to be carefully considered. Microfabrication of a standard Fabry-Perot (FP) cavity QCL starts by forming a laser cavity using dry or wet-etching to confine the current for low threshold. To passivate the cavity walls, there are two common approaches [1]; the first one is coating an electrically insulating material such as SiO_2 or Si_3N_4 on the mesa walls,

typically using PECVD, and the second is regrowth of an insulating epitaxial material, after the formation of the mesa with a semiconductor such as Fe doped InP, using MOCVD, to fill the trenches that form the cavity walls. Regrown material has the advantage of having low loss and thermal match with the epitaxial material. However, the fabrication of these buried heterostructure (BH) devices is complex and costly. Deposition and processing with SiO_2 or Si_3N_4 is a more accessible method, but these materials have relatively high optical absorption coefficient in the 8-12 μm wavelength region [2].

Many factors enter into consideration for the proper choice of a passivation layer. Both width and intensity of the vibrational mode leading to optical absorption of the passivating layer at the operating wavelength are high on the list. The degree of propagating mode overlap is also significant, as it is critical to the total absorbed power in the passivating layer. Finally, thermal resistance of the dielectric layer may also be expected to play a role. In previous works, low dissipation DFB devices with power consumption comparable to BH devices using AlN passivation were demonstrated [3], impact of optical constants and thermal conductivities of SiO_2 , Si_3N_4 and TiO_2 on the passivation of quantum cascade lasers were theoretically compared, and SiO_2 for short wavelengths and TiO_2 for long wavelengths into the midwave were recommended [4]. The feasibility of 15 μm wide 3 mm long e-beam evaporated Y_2O_3 thin film insulated double channel pulsed QCLs were demonstrated with reports of L-I-V curves, and it was concluded that SiO_2 and Si_3N_4 has significant absorption between 8 to 10 μm [5]. In another work, calculating the frequency dependent dielectric constants using Drude-Lorentz model, they studied the propagation of electromagnetic waves in various dielectrics to calculate absorption loss and optical confinement of QCL waveguides insulated with SiO_2 , Si_3N_4 , As_2S_3 , and $\text{Ge}_{0.25}\text{Se}_{0.75}$, and modeled using the finite element method [6]. In the latter work, SiO_2 and Si_3N_4 were compared with the low-loss materials using numerical analysis. However, loss difference between lasers with different passivation materials were not experimentally measured. HfO_2 has not been studied to date as a passivation material for QCLs.

Various approaches exist in the literature for measurement of loss in QCLs and similar semiconductor lasers. Those include the well-known Hakki-Paoli method [7], a generalized Hakki-Paoli method with Fourier analysis of sub-threshold electroluminescence [8] and analysis of current-power relationship [9], [10]. The first two rely on an analysis of electroluminescence spectrum of lasers driven at currents

S. Gündoğdu is with Physics Department, Bilkent University, Ankara 06800, Turkey

A. Demir is with UNAM - National Nanotechnology Research Center, Institute of Materials Science and Nanotechnology, Bilkent University, Ankara 06800, Turkey.

H. Sedaghat Pisheh is with Mechanical Engineering Department, Bilkent University, Ankara 06800, Turkey

A. Aydınli is with Electrical and Electronics Engineering Department, Uludağ University, Bursa, 16059 Turkey

below the lasing threshold. However, in a QCL, transition probabilities between the lasing energy levels depend on the applied voltage, hence, sub-threshold gain may be significantly different than the gain at the lasing voltage [11]. In the current-power analysis, the relationship between the cavity length and threshold current [10] or slope efficiency [9] is used to deduce the cavity loss. This method is preferred for its relative simplicity and for its ability to yield above-threshold loss. In this study, we compare FP cavity QCLs fabricated with PECVD grown Si_3N_4 and e-beam evaporated HfO_2 . We measured the slope efficiency and threshold currents of these lasers and from the relationship between the cavity length and slope efficiency, we calculated the cavity losses for two passivation materials. We also analyzed the optical losses for those materials, including the loss due to contact metals with 2D optical mode analysis using Comsol Multiphysics software.

II. EXPERIMENTAL

Laser crystals used in this study is similar to three phonon resonant scheme by Wang et. al [12]. Lattice matched layers are; 100nm InGaAs(5E18)/850nm InP(5E18)/2500nm InP (5E16)/200nm InGaAs (5E18)/2700nm Active region/200nm InGaAs(5E18)/2000nm InP(5E16)/50nm InGaAs(1E18)/Buffer InP (5E18)/Substrate InP(5E18). The numbers in the parentheses indicate Si doping levels. Two pieces with 1.5x1.5cm were cleaved from the same wafer. We formed the waveguides with 12, 16, 20 and 24 μm width by wet etching on both chips. One piece was coated with approximately 500 nm Si_3N_4 using PECVD with 180 sccm 2% SiH_4 in N_2 , 45 sccm NH_3 , 14W RF power, 400 mTorr pressure and 250°C substrate temperature. The other was coated with approximately 500 nm HfO_2 using e-beam evaporation with a rate of 0.3 nm/sec. Metallization contacts were formed by opening windows on the insulators on the top of the waveguides using buffered HF for both chips. Ti/Au (20/200 nm) for the top contacts and GeAu/Ni/Au (40/40/150 nm) for the bottom contacts were evaporated using e-beam. Top contacts were electroplated with 5 μm gold. Chips were cleaved into 1.8, 2.5 and 3.8 mm long waveguides and soldered on gold plated copper mounts with indium paste, epitaxial side up. Lasers were mounted in a liquid nitrogen cooled temperature controlled dewar with ZnSe window, heatsink temperature was set to -160°C. Voltage pulses of 1 μs width and 0.1% duty cycle were applied to the laser. Current through the lasers was measured through a series connected 1 Ω resistor using an oscilloscope. Optical power was measured using a gold integrating sphere with a fast HgCdTe photodetector connected to an oscilloscope. To measure absorption coefficient of Si_3N_4 and HfO_2 , 200 nm thick films were coated on infrared transparent silicon wafers. The extinction coefficient of the films were deduced from transmission measurement using an FTIR spectrometer.

III. RESULTS AND DISCUSSION

Optical peak power as a function of applied current for 24 μm wide and 2.5 mm long QC lasers is shown in Fig. 1a. Linear fits to the data is shown to guide the eye. Threshold

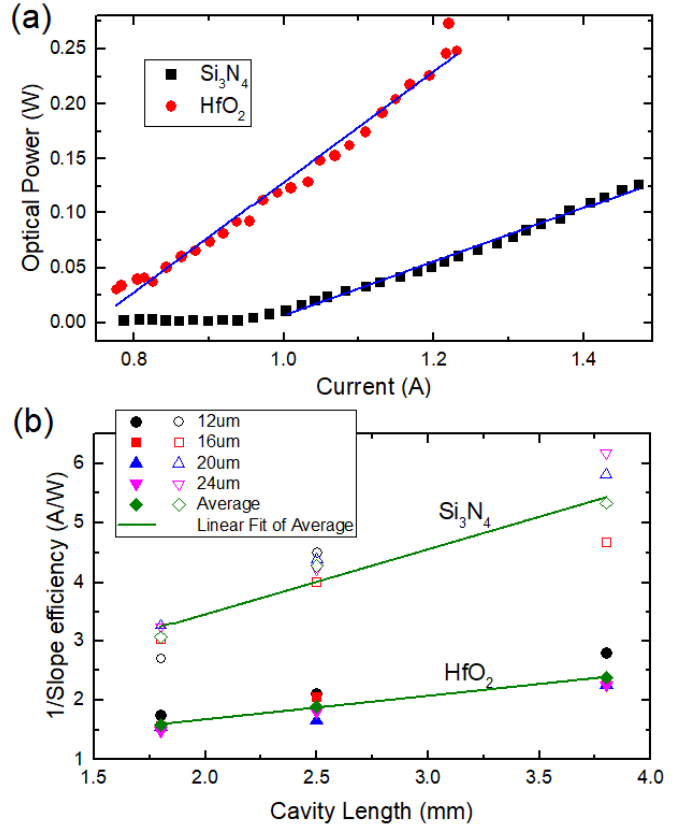


Fig. 1. Optical power as a function of current for 2.5 mm long 24 μm wide lasers passivated with Si_3N_4 and HfO_2 (a). Inverse slope efficiency as a function of cavity length (b). Si_3N_4 passivated lasers are shown with hollow symbols, HfO_2 passivated ones are shown with solid symbols. Waveguide widths are indicated in the inset. Average inverse slope efficiencies were calculated for each cavity length for both Si_3N_4 and HfO_2 . Linear fits to the average data are shown with solid lines.

currents were found from the intersection of the fitted lines with the current axis. Slope efficiencies were calculated from the slope of the linear fits. Threshold current for Si_3N_4 passivated laser is 1.00 A, and it drops to 0.75 A for HfO_2 passivated one. The slope efficiency of the lasers with HfO_2 is larger than those passivated with Si_3N_4 . We observed that this is the case for other lasers with different widths and lengths as well. Fig. 1b shows the inverse slope efficiency as a function of cavity length. Slope efficiencies of lasers with different widths are shown with different symbols. HfO_2 passivated lasers were labeled with hollow symbols and Si_3N_4 passivated ones were indicated with solid symbols. Diamond symbols shows the average of several inverse slope efficiency measurements for each passivation material and cavity length. Two linear fits were made to the average of inverse slope efficiency for the two passivation materials. The relationship between differential quantum efficiency, η_d , internal quantum efficiency, η_i , optical loss, α_i , and cavity length, L is given as [13];

$$\frac{1}{\eta_d} = \frac{\alpha_i}{\eta_i \ln(R_1 R_2)^{-1/2}} L + \frac{1}{\eta_i} \quad (1)$$

where R_1 and R_2 are back and front mirror reflectivities, which, in this case, are equal and $\approx 26\%$, since the effec-

tive index of the optical modes are ≈ 3.11 at the operating wavelength. Solid lines are linear fits to the average inverse slope efficiency for different waveguide widths. For HfO₂ passivated lasers, average optical loss of $6 \pm 0.5 \text{ cm}^{-1}$ and for Si₃N₄, $11.51 \pm 0.10 \text{ cm}^{-1}$ were measured. Fig. 2a shows the lasing

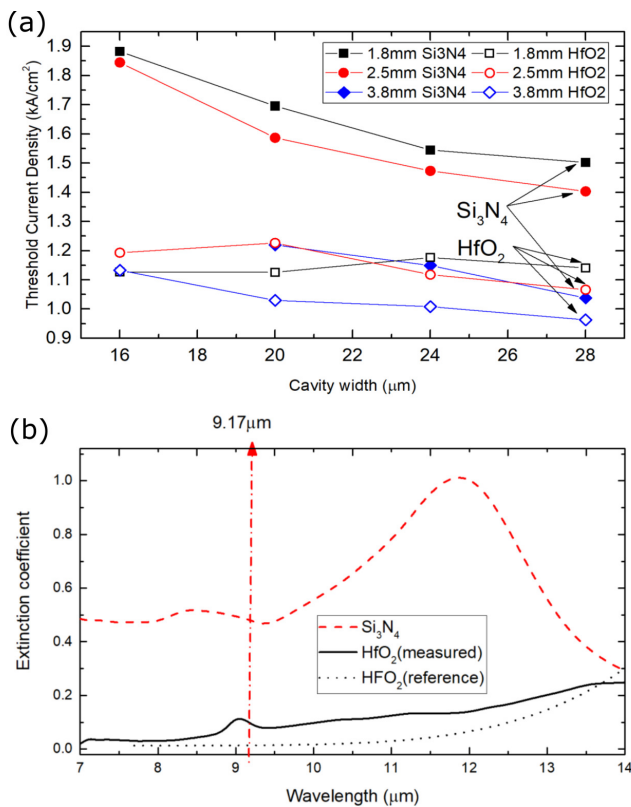


Fig. 2. Threshold current density as a function of cavity width for Si₃N₄ and HfO₂ passivation and different cavity lengths (a). Extinction coefficient measured using FTIR absorbance spectrum of Si₃N₄ and HfO₂ as a function of wavelength (b).

threshold current densities of the same lasers with Fig. 1, as a function of waveguide width. The threshold current density of Si₃N₄ lasers exhibits a strong dependency on waveguide width compared to HfO₂ lasers. This is due to the fact that, in narrower waveguides, optical mode overlap with the passivating dielectric is larger. Therefore, lasers with narrower waveguides are affected more by the optical loss due to the dielectric layer.

To compare the losses due to these two materials, we measured the absorbance spectrum of $\approx 200 \text{ nm}$ HfO₂ and Si₃N₄ films deposited on infrared transparent silicon. Since the film thickness is much less than the wavelengths of interest, the interference effects can be neglected, and Beer-Lambert law can be used to estimate the extinction coefficient;

$$1 - A = e^{-4\pi k z / \lambda} \rightarrow k = -\frac{\ln(1 - A)\lambda}{4\pi z} \quad (2)$$

where A is the absorbance, k is the extinction coefficient, z is the film thickness and λ is the wavelength. Measured extinction coefficients of the films are shown in Fig. 2b. The extinction coefficient of Si₃N₄ is much larger than that of

HfO₂ by a factor of 5 at the operating wavelength and peaks at around 11.5 μm due to the well-known Si-N vibrational modes. The extinction coefficient of HfO₂ is less than 0.1 for wavelengths shorter than 10 μm and it gets smaller towards shorter wavelengths. The central emission wavelength of our lasers, is at 9.17 μm , and indicated with a red dashed line. At these wavelengths, extinction coefficients are $k(\text{HfO}_2) = 0.095$ and $k(\text{Si}_3\text{N}_4) = 0.48$, and they differ by a factor of 5. In Fig. 2b, dashed black line is the extinction coefficient of magnetron sputtered HfO₂ reported by Bright et. al. [14]. This indicates that the extinction coefficient of HfO₂ film may even be smaller depending on the coating technique.

To examine the effect of optical loss due to dielectric and metal overcoat numerically, we used Comsol Multiphysics software, to model and calculate the complex effective index of the 2D waveguides for different mesa widths. We introduce extinction coefficient for the electroplated Au and the insulator in the form of a complex refractive index. As QCLs lase under TM polarization, we did the calculations only for the TM mode. Fig. 3a shows the geometry of the simulation when mesa width is 20 μm and Fig. 3b shows the corresponding fundamental mode. We varied the dielectric thickness between 50-1000 nm. From the imaginary part of the effective refractive index, we calculated the loss. Loss, as a function of dielectric thickness for various waveguide widths and dielectric thicknesses are indicated in Fig. 3c. There is a noticeable difference in optical loss between HfO₂ and Si₃N₄ passivation. For dielectric thicknesses below 300 nm loss due to gold overlayer significantly increases. Above 500 nm, loss converges to a value determined by the extinction coefficient of the insulator. For waveguide of 12 μm width with 500nm dielectric thickness, simulated loss difference between the two materials is 4 cm^{-1} , while the measured loss difference is 5.5 cm^{-1} . The small difference may be attributed to higher order optical modes which clearly experience higher losses. The simulated loss also increases as the mesa width decreases, which is consistent with our observation in Fig. 2a. These results are also in agreement with a recent study [5] which indicates that the loss of Si₃N₄ passivated lasers strongly depends on cavity width, compared to low-loss Y₂O₃ passivated ones. For wider waveguides, the difference in loss of the fundamental mode for two materials is smaller than 12 μm lasers, however, in wider lasers, the contribution of high order modes becomes prominent. Fig. 4a displays the first four of the TM mode electric field intensities of a 20 μm wide laser. TM0 is the fundamental TM mode and TM1, TM2, TM3 are the higher order modes. Fig. 4b shows the loss of the corresponding modes as a function of waveguide width. Loss of HfO₂ passivation is shown with dashed lines and loss of Si₃N₄ passivation is indicated with solid lines. Higher order modes have much higher losses due to larger mode overlap with the dielectric. Therefore, even for wide lasers, loss due to dielectric is significant as a result of high order modes.

IV. CONCLUSION

In conclusion, we have demonstrated an e-beam evaporated HfO₂ passivated QCL and measured its optical loss as well

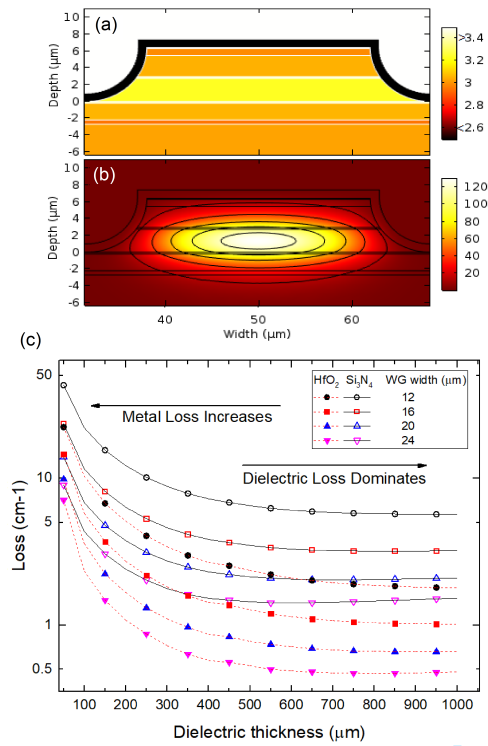


Fig. 3. The structure of the laser we modeled (a), and the calculated fundamental TM mode electric field (b). Calculated losses of the fundamental TM mode of lasers as a function of dielectric thickness (c). Waveguide widths are indicated in the inset. Losses in the case of Si_3N_4 passivation is shown with solid red lines and for HfO_2 is shown with dashed black lines.

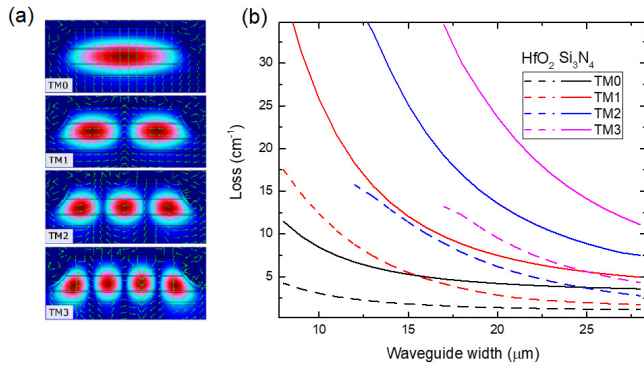


Fig. 4. Electric field intensity and vector map of four TM modes of $20\mu\text{m}$ wide laser (a), calculated loss for these modes for HfO_2 and Si_3N_4 passivation as a function of waveguide width.

as that of a PECVD grown Si_3N_4 passivated QCL. We have shown that loss for HfO_2 passivated lasers is almost half that of the Si_3N_4 passivated lasers and lasing threshold current densities are significantly less in the case of HfO_2 passivation. Our calculations show that the loss tends to decrease as the waveguides become wider, but even wider lasers have a significant dielectric loss due to high order modes. The thickness of the dielectric layer also plays an important role in the cavity loss and as the dielectric becomes thinner, plasmonic losses caused by the metal contacts increases. To reduce the loss for QCLs that lase in $8\text{--}12\mu\text{m}$ range, it is advisable to use

a low loss dielectric such as HfO_2 with approximately 500 nm thickness. This approach is both easy to implement and should lead to significant increase in the total optical power for all lasers operating in the $8\text{--}12\mu\text{m}$ region where sidewall passivation is required.

V. ACKNOWLEDGEMENTS

This project is supported by Republic of Turkey, Ministry of Science, Industry and Technology (Grant No: 573.STZ.2013-2).

We thank Prof. Carlo Sirtori for the QCL epitaxial design and valuable discussions and TÜBİTAK UME for loan of integrating sphere for optical power measurements.

REFERENCES

- [1] J. Faist, *Quantum Cascade Lasers*. Oxford University Press, 2013, p. 19.
- [2] J. Kischkat, S. Peters, B. Gruska, M. Semtsiv, M. Chashnikova, M. Klinkmüller, O. Fedosenko, S. Machulik, A. Aleksandrova, G. Monastyrskyi, Y. Flores, and W. T. Masselink, "Mid-infrared optical properties of thin films of aluminum oxide, titanium dioxide, silicon dioxide, aluminum nitride, and silicon nitride," *Applied Optics*, vol. 51, no. 28, p. 6789, sep 2012.
- [3] R. M. Briggs, C. Frez, M. Fradet, S. Forouhar, R. Blanchard, L. Diehl, and C. Pflügl, "Low-dissipation $74\text{-}\mu\text{m}$ single-mode quantum cascade lasers without epitaxial regrowth," *Optics Express*, vol. 24, no. 13, p. 14589, jun 2016.
- [4] S. Ferré, A. Peinado, E. Garcia-Caurel, V. Trinité, M. Carras, and R. Ferreira, "Comparative study of SiO_2 , Si_3N_4 and TiO_2 thin films as passivation layers for quantum cascade lasers," *Optics Express*, vol. 24, no. 21, p. 24032, oct 2016.
- [5] J. Kang, H.-D. Yang, B. S. Joo, J.-S. Park, S. ee Lee, S. Jeong, J. Kyhm, M. Han, J. D. Song, and I. K. Han, "Quantum cascade lasers with Y_2O_3 insulation layer operating at $8.1\mu\text{m}$," *Opt. Express*, vol. 25, no. 16, pp. 19561–19567, Aug 2017.
- [6] G. Rehouma, C. A. Evans, Z. Ikončić, D. Indjin, and P. Harrison, "Comparison of SiO_2 , Si_3N_4 , As_2S_3 , and $\text{Ge}_{0.25}\text{Se}_{0.75}$ dielectric layers for InP and GaAs based material systems for midinfrared quantum cascade laser waveguides," *Journal of Applied Physics*, vol. 106, no. 5, p. 053104, sep 2009.
- [7] B. W. Hakki and T. L. Paoli, "Gain spectra in GaAs double-heterostructure injection lasers," *Journal of Applied Physics*, vol. 46, no. 3, pp. 1299–1306, mar 1975.
- [8] D. Hofstetter and J. Faist, "Measurement of semiconductor laser gain and dispersion curves utilizing fourier transforms of the emission spectra," *IEEE Photonics Technology Letters*, vol. 11, no. 11, pp. 1372–1374, nov 1999.
- [9] J. Piprek, P. Abraham, and J. Bowers, "Cavity length effects on internal loss and quantum efficiency of multi-quantum-well lasers," *IEEE Journal of Selected Topics in Quantum Electronics*, vol. 5, no. 3, pp. 643–647, 1999.
- [10] C. Sirtori, P. Kruck, S. Barbieri, H. Page, J. Nagle, M. Beck, J. Faist, and U. Oesterle, "Low-loss al-free waveguides for unipolar semiconductor lasers," *Applied Physics Letters*, vol. 75, no. 25, pp. 3911–3913, dec 1999.
- [11] D. G. Revin, M. R. Soulby, J. W. Cockburn, Q. Yang, C. Manz, and J. Wagner, "Dispersive gain and loss in midinfrared quantum cascade laser," *Applied Physics Letters*, vol. 92, no. 8, p. 081110, feb 2008.
- [12] Q. J. Wang, C. Pflügl, L. Diehl, F. Capasso, T. Edamura, S. Furuta, M. Yamaniishi, and H. Kan, "High performance quantum cascade lasers based on three-phonon-resonance design," *Applied Physics Letters*, vol. 94, no. 1, p. 011103, jan 2009.
- [13] L. A. Coldren, S. W. Corzine, and M. L. Mašanović, *Diode Lasers and Photonic Integrated Circuits*. John Wiley & Sons, Inc., mar 2012, p. 75.
- [14] T. Bright, J. Watjen, Z. Zhang, C. Muratore, and A. Voevodin, "Optical properties of HfO_2 thin films deposited by magnetron sputtering: From the visible to the far-infrared," *Thin Solid Films*, vol. 520, no. 22, pp. 6793–6802, sep 2012.